# Interfacing Living Yeast Cells with Graphene Oxide Nanosheaths[a]

Sung Ho Yang,[b] Taemin Lee,[b] Eunyong Seo, Eun Hyea Ko, Insung S. Choi,*
Byeong-Su Kim*

The first example of the encapsulation of living yeast cells with multilayers of GO nanosheets via LbL self-assembly is reported. The GO nanosheets with opposite charges are alternatively coated onto the individual yeast cells while preserving the viability of the yeast cells, thus affording a means of interfacing graphene with living yeast cells. This approach is expanded by integrating other organic polymers or inorganic nanoparticles to the cells by hybridizing the entries with GO nanosheets through LbL self-assembly. It is demonstrated that incorporated iron oxide nanoparticles can deliver magnetic properties to the biological systems, allowing the integration of new physical and chemical functions for living cells with a combination of GO nanosheets.
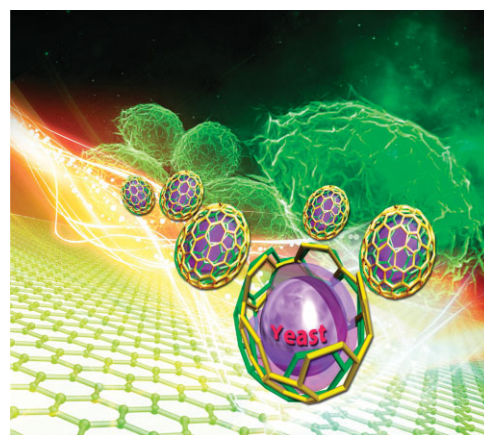
Introduction

Recent years have witnessed an emerging interest in biocompatible methods for interfacing biological systems with artificial materials, which have a great impact on the areas of single-cell-based sensors, neurons-on-a-chip, and tissue engineering. Unicellular microorganisms, such as bacteria, fungi, and algae, have been utilized extensively for the encapsulation of whole single cells as well as for the introduction of nanomaterials onto the living cells. For example, gold nanoparticles[1] and nanorods[2] were introduced onto the surface of Gram-positive bacteria by using specific interactions with the constituents of cell walls, and their utility for microelectronic devices was demonstrated. The layer-by-layer (LbL) self-assembly of polymers also has been used for encapsulating individual living cells with organic macromolecules.[3–9] In addition, the surface of microbial cells was doped with various nanoparticles, such as silica,[10,11] gold,[12] silver, and iron,[13] and carbon nanotubes[14] by the LbL self-assembly. Very recently, individual yeast cells were encapsulated within silica,[15,16] calcium phosphate,[17] calcium carbonate,[18] and polydopamine,[19] inspired by biomineralization processes or an adhesive protein found in mussels. On the other hand, a new strategy to the modification of cell surfaces by in vivo synthesis of diverse nanoparticles has been reported for certain types of bacterial cells[20] or recombinant bacterial cells.[21]

Although various nanoparticles and carbon nanotube were introduced on cell surfaces, such functional nano-

S. H. Yang, E. H. Ko, I. S. Choi
Molecular-Level Interface Research Center, Department of Chemistry, KAIST, Daejeon 305-701, Korea
E-mail: ischoi@kaist.ac.kr
T. Lee, E. Seo, B.-S. Kim
Interdisciplinary School of Green Energy and School of NanoBioscience and Chemical Engineering, Ulsan National Institute of Science and Technology (UNIST), Ulsan 689-798, Korea
E-mail: bskim19@unist.ac.kr

materials were utilized as dopants rather than as coating materials such as biominerals and macromolecules. We, hence, focused on graphene which has been attracting a great deal of attention because of its high electrical and thermal conductivities, mechanical properties, and large surface area.[22–24] We speculated that graphene could synergistically work not only for functional materials but also for coating materials for living cells, with a help of its sheets-like structure and flexible property.[25] Owing to these attributes, interfacing living cells with graphene can be useful for the integration of dynamic cellular physiology with electrical readouts.[26] Recently, several attempts have been made to interface graphene oxide (GO) with biomaterials: GO has been used for a membrane for DNA translocation,[27,28] quantitative measurement of the activity of helicase,[29] and a supportive material for cell culture.[30] Although these recent studies suggested the high potential of GO for biomaterials and biological systems, a tight interfacing of GO with whole living cells via encapsulation has not been attempted until now. In this paper, we report a simple, yet versatile method for encapsulating living yeast cells with GO shells.

Experimental Section

Materials

Poly(diallyldimethylammonium chloride) (PDDA, average $\overline{M}_w$: 100 000–200 000, 20 wt% in H_2O, Aldrich), poly(4-styrene sulfonate) (PSS, average $\overline{M}_w$: ≈70 000, powder, Aldrich), sodium phosphate dibasic (99%, Aldrich), and sodium dihydrogen phosphate (99%, Aldrich), graphite powder (Aldrich, <20 μm), iron(III) chloride hexahydrate (FeCl$_3 \cdot$6H$_2$O, Kanto chemical Co. Inc.), iron(II) chloride tetrahydrate (FeCl$_2 \cdot$4H$_2$O, Kanto Chemical Co. Inc.), tetramethylammonium hydroxide [(CH$_3$)$_4$NOH$\cdot$5H$_2$O, TMAOH, Aldrich] were used as received. Ultrapure water (18.2 MΩ·cm) from the Human Ultrapure System (Human Corp., Korea) was used.

Synthetic Procedures of GO Nanosheets

Negatively charged GO nanosheets (GO-COO$^-$) were synthesized from graphite powder (Aldrich, <20 μm) by the modified Hummers method and exfoliated to give a stable suspension of GO (typical concentration of 0.50 mg·mL^{-1}) under ultrasonication for 40 min and then centrifuged at 4000 rpm for 10 min to remove any aggregates remaining in the suspension. Positively charged GO nanosheets (GO-NH$_3^+$) were prepared by reacting GO-COO$^-$ with excess ethylenediamine under stirring for 5 h in the presence of N-ethyl-N'-(3-dimethylaminopropyl)carbodiimide methiodide (EDC, 98%, Alfa Aesar). The resulting suspension was dialyzed (molecular-weight cutoff 12 000–14 000, SpectraPore) for a few days to remove any by-products and residuals during functionalization. The prepared GO suspensions exhibited a fairly good colloidal stability over a wide span of pH conditions, and the pH of the suspension was adjusted to 7.4 prior to LbL assembly.

Synthetic Procedures of Fe$_3$O$_4$ Nanoparticles

Fe$_3$O$_4$ nanoparticles were prepared by the previous report.[31] A 5.4 g of FeCl$_3 \cdot$6H$_2$O (20 mmol), followed by 2.0 g of FeCl$_2 \cdot$4H$_2$O (10 mmol) was dissolved in a fresh solution of 25 mL of 0.40 M HCl. This solution was added dropwise to 250 mL of 1.5 M NaOH solution with vigorous stirring, which immediately formed a black precipitate. The precipitate was isolated via magnetic decantation and washed twice with water, and then twice with 0.1 M (CH$_3$)$_4$NOH$\cdot$5H$_2$O (TMAOH). Particles were separated by centrifugation (6000 rpm, 10 min) and the final precipitate was dissolved in 250 mL of 0.1 M TMAOH. The final, black, Fe$_3$O$_4$ nanoparticle solution was stored in air for further use.

Encapsulation with GO Nanosheets

A single colony of yeast cells was picked from a yeast extract/peptone/dextrose (YPD) broth agar plate, and suspended in the YPD broth and cultured in a shaking incubator at 30 °C for 30 h. The cells were washed with 0.15 M aqueous NaCl solution. The cells were alternately immersed in the suspensions of GO-NH$_3^+$ and GO-COO$^-$ for 5 min for each step. The LbL processes were started with GO-NH$_3^+$ for achieving electrostatic interactions with negatively charged cell surfaces. The cells were washed with 0.15 M aqueous NaCl solution after deposition of each step.

Encapsulation with GO Nanosheets, Polymers, and Fe$_3$O$_4$ Nanoparticles

Yeast@(PDDA$^+$/GO-COO$^-$) and yeast@(GO-NH$_3^+$/PSS$^-$) was formed by alternately immersing the native yeast cells in the suspensions of (PDDA$^+$/GO-COO$^-$) and (GO-NH$_3^+$/PSS$^-$) for 5 min for each step. Fe$_3$O$_4$-incorporated yeast@GO was generated by alternately immersing the native yeast cells in the suspensions of GO nanosheets and Fe$_3$O$_4$ nanoparticles. Finally, it gave the structure of yeast@(GO-NH$_3^+$/GO-COO$^-$/GO-NH$_3^+$/Fe$_3$O$_4^-$/GO-NH$_3^+$/Fe$_3$O$_4^-$).

Viability Test

The viability of yeast cells was measured by examining the activity of intracellular esterases and membranes integrity using fluorescein diacetate (FDA).[32,33] The stock solution (10 mg·mL^{-1}) was first prepared by dissolving FDA in acetone, because FDA was poorly soluble in water. The 2 μL of the stock solution was mixed with 1 mL of yeast cell suspension (10^{-2} M phosphate buffer solution, pH = 6.5). The suspension was incubated for 30 min at 37 °C while shaking, and then the cells were collected by centrifugation, washed with water, and characterized by confocal microscopy.

Characterization

Zeta-potential was measured with Zetasizer Nano ZS (Malvern, UK). The morphologies of the yeast@GO capsules were examined by transmission electron microscope (JEOL JEM-2100, Japan) and by field-emission scanning electron microscope (Sirion FEI XL FEG/ SFEG microscope, FEI Co., the Netherlands) with an accelerating voltage of 10 kV, after sputter-coating with platinum.

www.MaterialsViews.com

The cells were observed with an LSM 510 META confocal microscope (Carl Zeiss, Germany) and IX71 inverted microscope (Olympus, Japan).

Results and Discussion

We chose the LbL self-assembly as a method for introducing graphene on cell walls, based on our previous reports that the thin multilayer films of GO and reduced GO were formed on colloidal particles[34] as well as on the flat substrates[35,36] by the LbL self-assembly under physiologically mild conditions (e.g., aqueous solution or near neutral pH). Negatively charged GO nanosheets (GO-COO⁻) were prepared by following the modified Hummers method,[36] and positively charged one (GO-NH$_3^+$) by reacting GO-COO⁻ with ethylenediamine. The prepared GO suspensions exhibited a fairly good colloidal stability over a wide span of pH conditions, and the pH of the suspension was adjusted to 7.4 prior to LbL assembly. The yeast cells were encapsulated individually within the multilayers of GO-NH$_3^+$/GO-COO⁻ by repeatedly immersing the cells into the suspensions of GO-NH$_3^+$ and GO-COO⁻, to afford the encapsulated yeast cells [hereafter, yeast@GO$_{(n/m)}$, n = number of GO-NH$_3^+$ layers; m = number of GO-COO⁻ layers] (Scheme 1).

The multilayer deposition was initiated with positively charged GO-NH$_3^+$ nanosheet to enhance the electrostatic interaction because the native yeast cells were known to present highly negative charge.[15–17] It is obvious that deposition of oppositely charged GO nanosheet would change the surface charge of the yeast cells. The surface charge, therefore, was individually measured with the progress of the deposition of GO-NH$_3^+$ and GO-COO⁻ nanosheets on the yeast cells from the first layer to the fifth layer (Figure 1a). As a result, the zeta-potential values of yeast@GO periodically oscillated between positive and negative values after the deposition of the corresponding
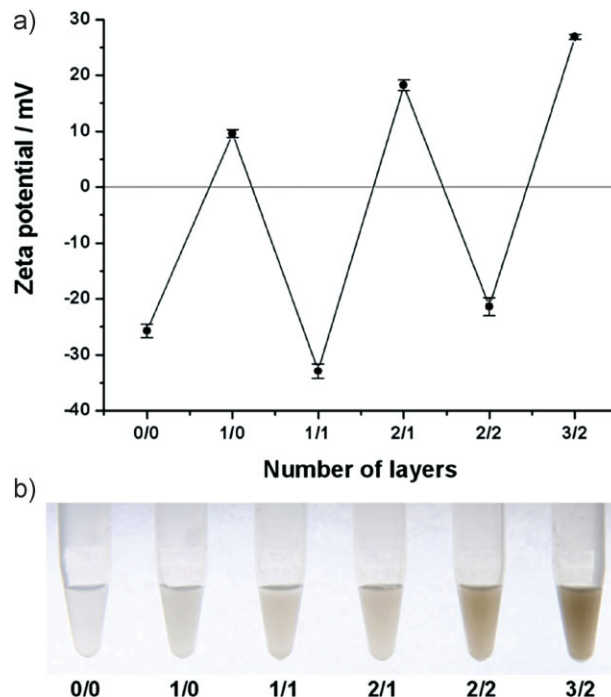

Figure 1. (a) Zeta-potentials and (b) corresponding optical images of yeast cells alternatively coated with multilayers of (GO-NH$_3^+$/GO-COO⁻)$_{(n/m)}$ as a function of layer number.

GO nanosheets, respectively. For instance, yeast@GO showed 9.6 ± 0.7 mV at the first adsorption of GO-NH$_3^+$ nanosheets, while native yeast exhibited a zeta-potential of -25.7 ± 1.2 mV.

These results of alternating surface charges are characteristic of colloidal particle-based LbL assembly, implying that yeast cells are sequentially coated with oppositely charged GO nanosheets based on electrostatic interaction. In addition, the color of suspension of yeast@GO became darker as the number of deposition cycle increased (Figure 1b). This observation can be explained by the

Scheme 1. Encapsulation of yeast cell within GO nanosheets via LbL self-assembly.

inherent nature of graphene-related materials; single layer of graphene is nearly transparent to the visible light but stacks or suspension of graphene are dark brown. For example, the transmittance of GO multilayered thin films formed on glass substrates by LbL self-assembly decreased gradually with increasing number of layer of GO nanosheets, as demonstrated in our previous report.[35] Taken together, we found that we could successfully control the deposition of GO nanosheets onto the biological surface by taking advantages of the LbL self-assembly in nanoscale surface engineering.

On the basis of the stable deposition of GO multilayers onto the native yeast cells, the morphology of native yeast and yeast@GO was investigated by means of scanning electron microscopy (SEM, Figure 2a,b). The SEM micrographs clearly confirmed the single-cell encapsulation of yeast cells within GO nanosheets. Interestingly, yeast@GO preserved the original round shape of yeast, whereas the native yeast became highly shrunk due to dehydration

during the sample preparation. High-magnification SEM further provides the characteristic wrinkled surface of GO nanosheet, which reflects a flexible nature of GO nanosheet that can be beneficial to cover the biological surfaces in a conformable manner. The crumpled structure of GO nanosheets was similarly observed on the polystyrene colloids decorated with GO sheets, but the crease was not as pronounced as that on yeast cells.[34] This difference is mainly attributed to the dehydration effect; collapsed inner cell structure upon dehydration resulted in more crumpled GO nanosheet structures, but polystyrene colloids did not suffer from dehydration after the assembly. Transmission electron microscopy (TEM) images also clearly confirmed GO shells and displayed the characteristic surface of GO on top of yeast cell (Figure 2c,d). In addition, yeast@GO in an aqueous suspension was further observed with confocal microscopy (see Supporting Information). Confocal micrographs confirmed that yeast cells are individually encapsulated and maintained their original shapes even after GO encapsulation.

Addressing the biocompatibility of artificial materials or modification protocols would be an essential prerequisite for utilization of the materials or protocols applicable for biological systems of interests. Although GO has been successfully utilized as a supportive material for culturing fibroblast cells,[29] biocompatibility of GO introduced onto whole living cells has not been investigated to date. We, therefore, investigated the viability of yeast@GO by using FDA, which examined the activity of intracellular esterases and emitted green fluorescence by reactive oxygen species; yeast cells in green were considered alive, and the others were considered dead.[16,18,19] Viability test indicated that the GO nanosheet encapsulation was compatible with living yeast cells as shown in Figure 2. Moreover, the permeability to FDA implied that GO multilayer shell would be permeable to small molecules such as water or nutrients. This is an interesting feature of GO compared to pristine graphene that is not permeable to other nutrients in its pristine condition. By referencing the viability of the native yeast as 100%, we determined the viability of yeast@GO was around 67% based on counting more than 200 yeast cells. The decreased viability could be explained by physical stress introduced during the LbL assembly such as centrifugation and vortex cycles and/or chemical stress from highly charged GO nanosheets in the solution. This was in accordance with our previous works on the silica[15] and polydopamine[19] encapsulated yeast cells which indicated that the initial viability was about 70% after encapsulation processes. We believe that the observed viability would be relatively high enough for the use of GO nanosheet as an encapsulation material. In addition to the FDA-based viability assay, we also conducted another fluorescent dye-based assay using resarufin (Promega Biosciences, Inc), which indicated a similar degree of cell
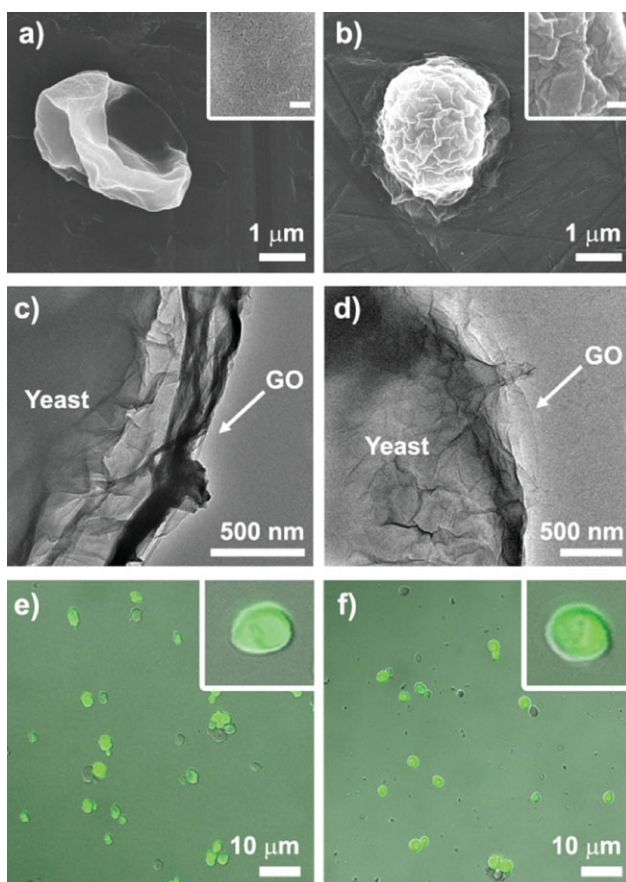

Figure 2. (a,b) SEM micrographs and (c,d) TEM micrographs, and (e,f) confocal fluorescence microscope images of (a,e) native yeast and (b,c,d,f) yeast@GO$_{(3/2)}$. Insets in (a) and (b) show the surface morphologies of each yeast cell. The scale bar in inset: 100 nm. The yeast cells are observed in aqueous suspensions, after staining with FDA for viability tests.

www.MaterialsViews.com

viability (see Supporting Information). Furthermore, we treated the yeast@GO with rhodamine dye, which can selectively adsorb on the graphene nanosheets via π-π interactions. The rhodamine-adsorbed yeast@GO showed the bright red fluorescence from rhodamine bound on the periphery of GO nanosheet, while the green fluorescence from FDA was also arising from the viable yeast cell within the capsule (see Supporting Information). This observation confirmed the successful integration of graphene nanosheath around the living yeast cell. Moreover, the integrated graphene nanosheath will provide potentials of introducing hydrophobic aromatic drugs and/or DNA for selective drug and gene delivery of graphene nanosheath to the encapsulated cells.

Finally, in order to demonstrate the versatility of our LbL approach toward the encapsulation of living cells, we have expanded the toolbox to other organic polyelectrolytes and nanoparticles for encapsulation of yeast cell. Organic polymers and inorganic nanoparticles can bring various new functionalities to the cell membranes, including fluorescent and magnetic property, catalytic moieties, and supporting templates.[11–19] For that, we have attempted to assemble multilayers on the yeast cells with a combination of GO nanosheets with two most common strong polyelectrolytes such as $PDDA^+$, and PSS^-. According to the same protocol, the yeast cells were encapsulated based on the electrostatic interactions between oppositely charged GO nanosheets and organic polyelectrolytes in a format of yeast@$(PDDA^+/GO-COO^-)$ and yeast@$(GO-NH_3^+/PSS^-)$, respectively. The SEM micrographs confirmed that
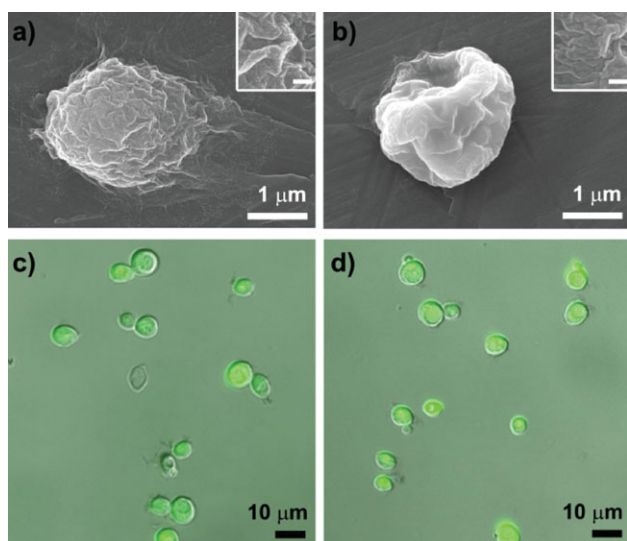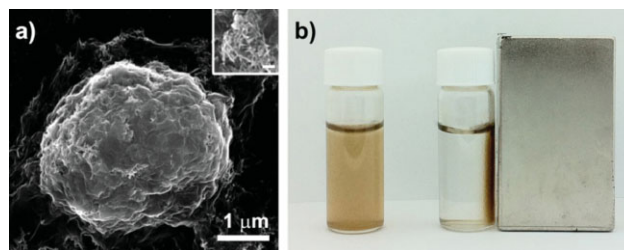
Figure 4. (a) SEM micrographs and (b) optical images of Fe_3O_4-incorporated yeast@GO. Inset figures in (a) show the surface morphologies of each yeast cell. The scale bar in the inset is 100 nm. Fe_3O_4-incorporated yeast@GO is randomly distributed in the suspension (left). In contrast, cells are concentrated around a magnet by magnetic interactions (right).

the yeast cells were individually encapsulated within multilayers composed of GO nanosheets and polymers (Figure 3a,b). The high-magnification images also displayed the crumpled nature of GO nanosheets, as similarly observed with yeast@GO. Green fluorescence in yeast cell stained by FDA indicated that the hybridized multilayers of GO nanosheets with polymers are biocompatible for encapsulating microbial cells (Figure 3c,d). In addition, we introduced magnetism to the yeast cells by incorporating negatively charged Fe_3O_4 nanoparticles in GO nanosheets as one component during the LbL assembly, in a format of yeast@$(GO-NH_3^+/GO-COO^-/GO-NH_3^+/Fe_3O_4^-/GO-NH_3^+/Fe_3O_4^-)$. SEM micrographs confirmed that Fe_3O_4 nanoparticles were successfully incorporated within GO nanosheets (Figure 4a). Furthermore, we found that the Fe_3O_4-incorporated yeast@GO was driven by a magnetic force and we could concentrate the cells around a magnet (Figure 4b). We expect that incorporation of magnetism into cells would be beneficial for collecting and identifying living cells.[37,38] Collectively, these demonstrations imply that the GO multilayers can be utilized as scaffolds for introducing advantageous physical and chemical functions for living cells.

Conclusion

In summary, we formed a nanosheath of GO on individual yeast cells by selectively depositing GO nanosheets via LbL self-assembly. This study elucidated that GO is biocompatible to the yeast cells and LbL self-assembly would be highly suitable for introducing graphene and related carbon nanomaterials to the biological systems in a controllable way without significantly sacrificing the viability. The field of interfacing individual living cells with nanomaterials is still in its infancy, but we anticipate that the results presented in this study would provide a basis for the application of biological systems to achieve biosensors, biomedical devices, and tissue engineering, by taking

Figure 3. (a,b) SEM micrographs and (c,d) confocal fluorescence microscope images of (a,c) yeast@$PDDA^+/GO^-_{(5/5)}$, and (b,d) yeast@$GO^+/PSS^-_{(5/4)}$. Inset figures in (a) and (b) show the surface morphologies of each yeast cell. The scale bare in inset: 100 nm. The yeast cells are observed in aqueous suspensions, after staining with FDA for viability tests.

Materials
Views
www.MaterialsViews.com

Macromol. Biosci. **2012**, *12*, 61–66
© 2012 WILEY-VCH Verlag GmbH & Co. KGaA, Weinheim

Macromolecular
Journals

65

advantage of extraordinary physical properties of graphene together with the versatility of LbL self-assembly.

[1] V. Berry, S. Rangaswamy, R. F. Saraf, *Nano Lett.* **2004**, *4*, 939.
[2] V. Berry, A. Gole, S. Kundu, C. J. Murphy, R. F. Saraf, *J. Am. Chem. Soc.* **2005**, *127*, 17600.
[3] V. Kozlovskaya, S. Harbaugh, I. Drachuk, O. Shchepelina, N. Kelley-Loughnane, M. Stone, V. V. Tsukruk, *Soft Matter* **2011**, *7*, 2364.
[4] N. G. Veerabadran, P. L. Goli, S. S. Stewart-Clark, Y. M. Lvov, D. K. Mills, *Macromol. Biosci.* **2007**, *7*, 877.
[5] A. L. Hillberg, M. Tabrizian, *Biomacromolecules* **2006**, *7*, 2742.
[6] S. Krol, M. Nolte, A. Diaspro, D. Mazza, R. Magrassi, A. Gliozzi, A. Fery, *Langmuir* **2005**, *21*, 705.
[7] A. Diaspro, D. Silvano, S. Krol, O. Cavalleri, A. Gliozzi, *Langmuir* **2002**, *18*, 5047.
[8] J. T. Wilson, W. Cui, V. Kozlovskaya, E. Kharlampieva, D. Pan, Z. Qu, V. R. Krishnamurthy, J. Mets, V. Kumar, J. Wen, Y. Song, V. V. Tsukruk, E. L. Chaikof, *J. Am. Chem. Soc.* **2011**, *133*, 7054.
[9] J. L. Carter, I. Drachuk, S. Harbaugh, N. Kelley-Loughnane, M. Stone, V. V. Tsukruk, *Macromol. Biosci.* **2011**, *11*, 1244.
[10] H. Ai, M. Fang, S. A. Jones, Y. M. Lvov, *Biomacromolecules* **2002**, *3*, 560.
[11] S. S. Balkundi, N. G. Veerabadran, D. M. Eby, G. R. Johnson, Y. M. Lvov, *Langmuir* **2009**, *25*, 14011.
[12] R. F. Fakhrullin, A. I. Zamaleeva, M. V. Morozov, D. I. Tazetdinova, F. K. Alimova, A. K. Hilmutdinov, R. I. Zhdanov, M. Kahraman, M. Culha, *Langmuir* **2009**, *25*, 4628.
[13] R. F. Fakhrullin, L. V. Shlykova, A. I. Zamaleeva, D. K. Nurgaliev, Y. N. Osin, J. Garcia-Alonso, V. N. Paunov, *Macromol. Biosci.* **2010**, *10*, 1257.
[14] A. I. Zamaleeva, I. R. Sharipova, A. V. Porfireva, G. A. Evtugyn, R. F. Fakhrullin, *Langmuir* **2010**, *26*, 2671.
[15] S. H. Yang, K. B. Lee, B. Kong, J. H. Kim, H. S. Kim, I. S. Choi, *Angew. Chem., Int. Ed.* **2009**, *48*, 9160.
[16] S. H. Yang, E. H. Ko, Y. H. Jung, I. S. Choi, *Angew. Chem., Int. Ed.* **2011**, *50*, 6115.
[17] B. Wang, P. Liu, W. G. Jiang, H. H. Pan, X. R. Xu, R. K. Tang, *Angew. Chem., Int. Ed.* **2008**, *47*, 3560.
[18] R. F. Fakhrullin, R. T. Minullina, *Langmuir* **2009**, *25*, 6617.
[19] S. H. Yang, S. M. Kang, K.-B. Lee, T. D. Chung, H. Lee, I. S. Choi, *J. Am. Chem. Soc.* **2011**, *133*, 2795.
[20] W. S. Kuo, C. M. Wu, Z. S. Yang, S. Y. Chen, C. Y. Chen, C. C. Huang, W. M. Li, C. K. Sun, C. S. Yeh, *Chem. Commun.* **2008**, 4430.
[21] T. J. Park, S. Y. Lee, N. S. Heo, T. S. Seo, *Angew. Chem., Int. Ed.* **2010**, *49*, 7019.
[22] K. S. Novoselov, A. K. Geim, S. V. Morozov, D. Jiang, Y. Zhang, S. V. Dubonos, I. V. Grigorieva, A. A. Firsov, *Science* **2004**, *306*, 666.
[23] K. S. Novoselov, A. K. Geim, S. V. Morozov, D. Jiang, M. I. Katsnelson, I. V. Grigorieva, S. V. Dubonos, A. A. Firsov, *Nature* **2005**, *438*, 197.
[24] Z. S. Wu, W. C. Ren, L. B. Gao, J. P. Zhao, Z. P. Chen, B. L. Liu, D. M. Tang, B. Yu, C. B. Jiang, H. M. Cheng, *ACS Nano* **2009**, *3*, 411.
[25] J. Hong, J. Y. Han, H. Yoon, P. Joo, T. Lee, E. Seo, K. Char, B.-S. Kim, *Nanoscale*, DOI: 10.1039/C1NR10575B.
[26] R. Kempaiah, A. Chung, V. Maheshwari, *ACS Nano* **2011**, *5*, 6025.
[27] C. A. Merchant, K. Healy, M. Wanunu, V. Ray, N. Peterman, J. Bartel, M. D. Fischbein, K. Venta, Z. T. Luo, A. T. C. Johnson, M. Drndic, *Nano Lett.* **2010**, *10*, 2915.
[28] G. F. Schneider, S. W. Kowalczyk, V. E. Calado, G. Pandraud, H. Zandbergen, L. M. K. Vandersypen, C. Dekker, *Nano Lett.* **2010**, *10*, 3163.
[29] H. Jang, Y. K. Kim, H. M. Kwon, W. S. Yeo, D. E. Kim, D. H. Min, *Angew. Chem., Int. Ed.* **2010**, *49*, 5703.
[30] S. R. Ryoo, Y. K. Kim, M. H. Kim, D. H. Min, *ACS Nano* **2010**, *4*, 6587.
[31] J. L. Lyon, D. A. Fleming, M. B. Stone, P. Schiffer, M. E. Williams, *Nano Lett.* **2004**, *4*, 719.
[32] W. Jakubowski, G. Bartosz, *Int. J. Biochem. Cell Biol.* **1997**, *29*, 1297.
[33] P. Breeuwer, J.-L. Drocourt, N. Bunschoten, M. H. Zwietering, F. M. Rombouts, T. Abee, *Appl. Environ. Microbiol.* **1995**, *61*, 1614.
[34] J. Hong, K. Char, B.-S. Kim, *J. Phys. Chem. Lett.* **2010**, *1*, 3442.
[35] D. W. Lee, T. K. Hong, D. Kang, J. Lee, M. Heo, J. Y. Kim, B. S. Kim, H. S. Shin, *J. Mater. Chem.* **2011**, *21*, 3438.
[36] T. K. Hong, D. W. Lee, H. J. Choi, H. S. Shin, B. S. Kim, *ACS Nano* **2010**, *4*, 3861.
[37] J. García-Alonso, R. F. Fakhrullin, V. N. Paunov, *Biosens. Bioelectron.* **2010**, *25*, 1816.
[38] R. F. Fakhrullin, J. García-Alonso, V. N. Paunov, *Soft Matter* **2010**, *6*, 391.